Front. Optoelectron. 2016, 9(2): 238–248
DOI 10.1007/s12200-016-0621-4

REVIEW ARTICLE

Microwave photonics connected with microresonator frequency combs

Xiaoxiao XUE (✉)[1], Andrew M. WEINER (✉)[1,2]

1 School of Electrical and Computer Engineering, Purdue University, 465 Northwestern Avenue, West Lafayette, Indiana 47907-2035, USA
2 Birck Nanotechnology Center, Purdue University, 1205 West State Street, West Lafayette, Indiana 47907, USA

Abstract Microresonator frequency combs (microcombs) are very promising as ultra-compact broadband sources for microwave photonic applications. Conversely, microwave photonic techniques are also employed intensely in the study of microcombs to reveal and control the comb formation dynamics. In this paper, we reviewed the microwave photonic techniques and applications that are connected with microcombs. The future research directions of microcomb-based microwave photonics were also discussed.

Keywords microwave photonics, optical frequency comb, microresonator, Kerr effect, four-wave mixing

1 Introduction

Microresonator based optical frequency comb (often termed "microcomb" or "Kerr comb") generation was first demonstrated in 2007 [1]. It quickly attracted people's great interest and evolved to a hot research area. Microcombs are very promising for portable applications because they have many unique advantages including the capability of generating ultra-broad comb spectra (even more than one octave [2,3]), chip-level integration [4,5], and low power consumption. The basic scheme of microcomb generation is shown in Fig. 1(a). The frequency of a pump laser is tuned into the resonance of one high-quality-factor (Q) microresonator which is made of Kerr nonlinear material. When the pump power exceeds some threshold, new frequency lines grow due to parametric gain. More lines are generated through cascaded four-wave mixing between the pump and initial lines, forming a broad frequency comb [6]. Intense studies have been performed to investigate microcomb generation. Various materials and microresonator structures have been exploited, including whisper-gallery-mode (WGM) microresonators made of silica [1], fused quartz [7], fluoride crystalline [8–10], and sapphire [11]; planar waveguide microrings made of silicon nitride [4], Hydex glass [5], aluminum nitride [12], diamond [13], and silicon [14]. Microcomb generation is a hopeful candidate that may bring revolutionary changes to the frequency comb applications. Many pioneering demonstrations have been reported [15–23]; some of them fall in the category of microwave photonics, such as high-spectral-purity microwave generation [21] and microwave photonic signal processing [22,23].

The research of microwave photonics can date back to 1960s, nearly as early as when the first laser source was invented [24] and fast light modulation and detection techniques were developed [25,26]. The aim of microwave photonics is using photonic devices to achieve microwave functions which are difficult or impossible for electronic techniques. Promising microwave photonic applications include microwave oscillators, signal processing, antenna beam steering, analog transmission, arbitrary waveform generation, and analog-to-digital convertor. Recent advances in these fields have been summarized by several nice review papers [27–34]. The potential advantages of microwave photonic technology include large bandwidth, low transmission loss, fast tunability, high reconfigurability, and immunity to electro-magnetic interference. For example, compared to coaxial cable links, radio-over-fiber links which have been commercially established show outstanding performances in terms of bandwidth, transmission loss, cost and volume. However, for the other microwave photonic applications, there are still many drawbacks, mainly the bulk volume, high cost and high power consumption which makes it difficult for them to compete with well-developed integrated microwave and millimeter-wave circuits. To address these problems,

Received February 1, 2016; accepted February 18, 2016

E-mails: xue40@purdue.edu, amw@purdue.edu

integrated microwave photonics is now becoming a new developing direction [32–34].

Optical frequency combs have emerged in recent years as an important element in the research of microwave photonics. An optical frequency comb is often regarded as a source that links optical frequency and microwave frequency. The frequency of each comb line is hundreds of THz, while the comb line spacing is generally in the microwave range (MHz ~ GHz). Figure 1(b) illustrates an optical frequency comb working in optical clocks as a gear that converts optical frequency to microwave frequency [35]. Traditional optical frequency combs are based on mode-locked lasers [36] or electro-optic modulation [37]. The systems generally have high complexity and large volume. In comparison, integrated microcombs can provide compact volume and low power consumption, thus are very promising to bring comb-based microwave photonic systems to real-world applications. Interestingly, the microwave photonic techniques are also employed intensely in the study of microcombs to reveal and control the comb formation dynamics. In this paper, we will review the microwave photonic techniques and applications that are connected with microcombs. The rest of this paper is organized as follows: Section 2 introduces the microwave photonic techniques that are useful in the study of microcombs, including inferring the effective detuning by detecting the Pound–Drever–Hall (PDH) signal, measuring the microresonator coupling condition by transferring the optical transmission spectrum to the microwave domain, and tuning the comb line spacing through external parametric seeding; Section 3 summarizes the microwave photonic demonstrations based on microcombs, including high-spectral-purity microwave generation and microwave photonic signal processing; finally in Section 4 we discuss the opportunities and future research directions for microcomb-based microwave photonics.

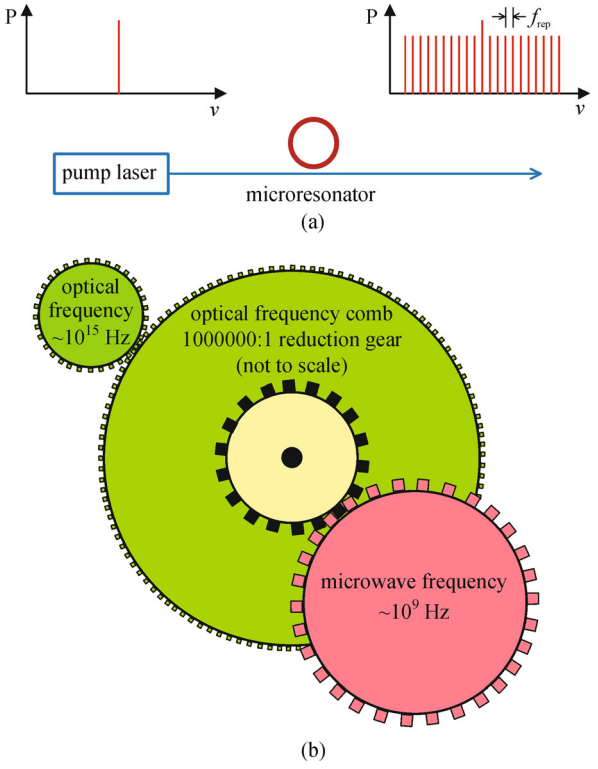

Fig. 1 (a) Illustration of microresonator based optical frequency comb generation. A single pump frequency is converted to a broadband frequency comb by using a high-Q nonlinear microresonator. The comb line spacing (f_{rep}) is determined by the free spectral range of the microresonator which is usually in the microwave frequency range; (b) optical frequency comb working as a gear that links optical frequency and microwave frequency (adapted from Ref. [35])

2 Microwave photonics for microcomb generation

2.1 Pound–Drever–Hall technique

The frequency detuning between the pump laser and the microresonator resonance is an important factor that affects the comb formation dynamics. However, it is not straightforward to tell the detuning based on the cold-cavity transmission spectrum under comb generation conditions. The strong Kerr effect and thermal-optic effect cause resonance shifting to longer wavelength which is difficult to calibrate [38]. The PDH detection can be employed to monitor the effective detuning between the pump laser and the shifted resonance.

The PDH technique is widely used for stabilizing a laser frequency by locking it to a stable reference cavity [39,40]. The detuning between the laser frequency and the cavity is indicated by a voltage which is generally called the PDH error signal. The scheme of PDH detection is shown in Fig. 2(a), with its principle shown in the inset. The phase of the laser is modulated by a single-frequency microwave source before the microresonator. The microwave frequency is generally higher than the resonance width of the cavity. Two modulation sidebands namely the upper and lower sidebands are generated after phase modulation. Before passing through the microresonator, the beat note of the carrier and upper sideband has a π-phase shift compared to that of the carrier and lower sideband. They cancel each other thus no microwave oscillation can be detected by sending the light to a photodetector (recall that this is phase modulation). After passing through the microresonator, the phase of the carrier is shifted by the cavity response when the laser frequency is close to the resonance (the amplitude is also changed). This breaks the π-phase shift between the two beat notes corresponding to the upper and lower sidebands, and converts the phase modulation to intensity modulation. A microwave signal can then be detected and subsequently down-converted to a dc voltage by mixing with the microwave source. Figure 2(b) shows the typical results when the laser frequency scans across the resonance

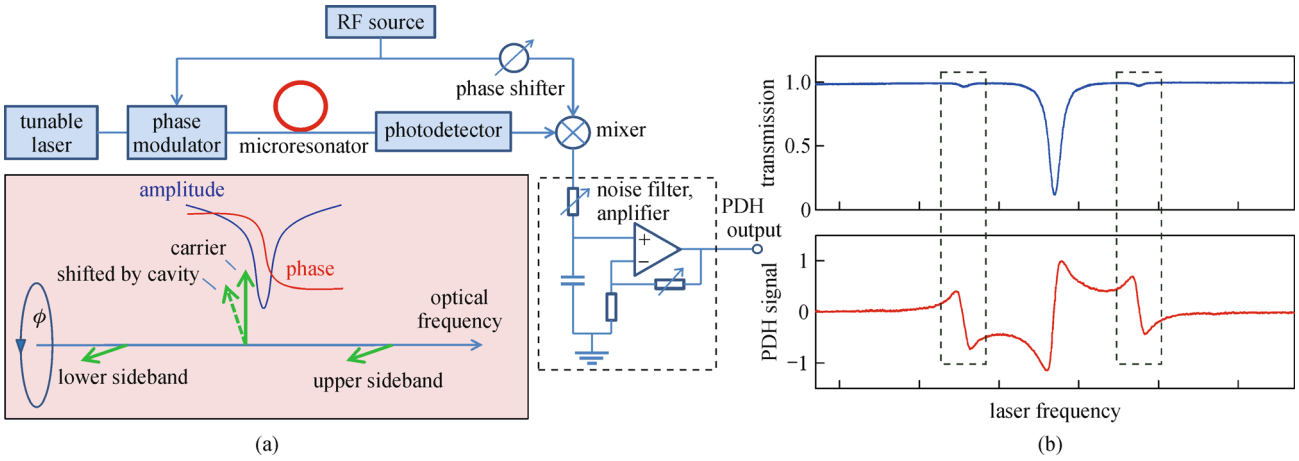

Fig. 2 (a) Scheme of PDH signal detection. The inset illustrates how the phase modulation is converted to intensity modulation after the light passes through the microresonator; (b) example PDH signal detected for a microring resonator. Upper: optical power after the microresonator; lower: PDH signal. The small dips and ripples marked in dash boxes are due to the sidebands scanning across the resonance

with a low power (thus no observable nonlinear effect and thermal effect). It can be seen that the PDH voltage is negative/positive when the laser frequency is lower/higher than the resonance frequency (the small dips and ripples marked in dash boxes are due to the sidebands scanning across the resonance). The detuning value can also be inferred from the PDH voltage. Note that the polarity of the PDH signal can be switched by tuning the phase shifter in Fig. 2(a).

In Ref. [41], the PDH signal is detected to diagnose whether the pump laser is blue detuned (laser frequency higher than resonance frequency) or red detuned with respect to the resonance. An MgF_2 WGM microresonator (loaded $Q \sim 4 \times 10^8$) which has anomalous group velocity dispersion is pumped for comb generation. The pump laser frequency is scanned from the blue side and across the resonance. Due to Kerr nonlinearity and thermo-optic effect, the resonance shifts to the red direction following the laser frequency, resulting in a typical triangular power transmission curve as shown in Fig. 3(a). Several power steps are observed around the end of the triangular shape. The PDH signal indicates that the effective detuning of the pump laser changes from blue to red after the first power step, as shown in Fig. 3(b). Together with the detuning change, the comb transitions from a high-noise incoherent state to a low-noise mode-locked state. Time-domain measurements show that temporal microresonator solitons are formed in the effective red detuning region. The small power steps after the detuning transition correspond to different number of solitons in the cavity. An example of smooth comb spectrum related to a single soliton in the cavity is shown in Fig. 3(c). The detuning information revealed by the PDH signal is very helpful for understanding the soliton formation dynamics and may inspire new experimental techniques to generate soliton combs. One interesting thing here is that the microwave modulation frequency is much higher than the resonance width; thus the sidebands fall out of the resonance without affecting the comb dynamics. It should also be noted that although the sign of the effective detuning can be learned easily from the sign of the PDH signal, it is difficult to get the detuning magnitude from the PDH signal. The pump line under comb generation conditions is subjected to a nonlinear loss due to power transfer to the other comb lines, resulting in a degraded effective quality factor of the cavity. The magnitude of effective pump detuning can be retrieved by following the procedure introduced in the supplementary section of Ref. [42].

2.2 Microresonator coupling condition test

The microresonator is coupled to an external waveguide for pump injection and comb extraction. The intrinsic losses of the light traveling in a microresonator generally include absorption loss and scattering loss. The external coupling introduces an additional loss and reduces the microresonator Q factor. When the coupling loss is lower/higher/equal than/to the intrinsic cavity loss, the microresonator is called under-/over-/critically coupled. The microresonator coupling condition is an important factor that affects the pump power threshold for comb generation and the power conversion efficiency (i.e., how much power is transferred from the pump to the new frequency lines). It has been found that the minimum threshold for comb generation requires the microresonator to be slightly under-coupled while higher efficiency can be achieved when the microresonator is over-coupled [1,43,44].

The coupling condition cannot be completely learned by measuring the microresonator power transmission spectrum, as two microresonators may have the same transmission amplitude but one is under-coupled and the other is over-coupled. The under-/over- coupling condi-

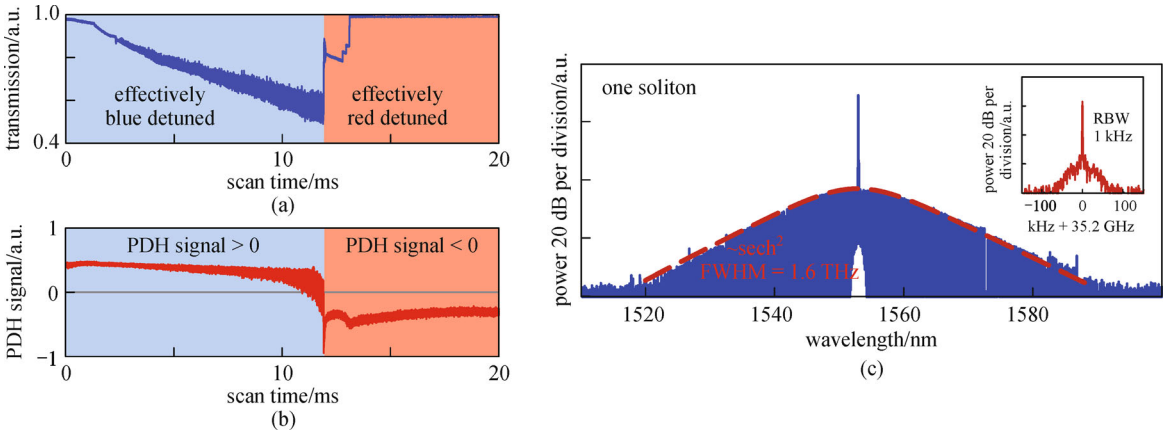

Fig. 3 Diagnosing the effective detuning in comb generation by detecting the PDH signal. The pump laser frequency scans across the resonance from the blue side (i.e., laser frequency higher than resonance frequency). (a) Optical power after the microresonator; (b) PDH signal. The PDH signal changes polarity at ~12 ms indicating a change of the effective detuning from blue to red; (c) a smooth frequency comb generated in the effectively red detuned region corresponding to a single bright soliton propagating in the microresonator. The inset shows the narrow-linewidth beat note of adjacent comb lines (adapted by permission from Macmillan Publishers Ltd: Nature Photonics [41], copyright 2014). FWHM: full-width at half-maximum; RBW: resolution bandwidth

tions can be distinguished from the phase response of the transmission spectrum. A method of measuring the microresonator phase response was proposed in the supplementary section of Ref. [42]. The scheme is shown in Fig. 4(a). The frequency of a tunable laser is tuned close to the resonance of the microresonator. The laser is modulated by a microwave signal through single-sideband modulation. By sweeping the microwave frequency, the sideband sweeps across the resonance. The response of the microresonator is then transferred to the electrical domain through beating of the sideband with the carrier. Figures 4(b) and 4(c) show two examples of the measured results for two microresonators which are over-coupled and under-coupled respectively. Different phase response curves can be observed. After the coupling condition is known, the intrinsic cavity loss and the coupling loss can be retrieved by fitting the power transmission spectrum.

The information of coupling condition is also required when the intracavity time-domain waveform is characterized based on measurements performed at the through port. The pump line at the through port is coherent summation of the pump from the input port and the component from the cavity. It can be corrected to estimate the intracavity complex pump field by following the procedure proposed in Ref. [42]. The cold-cavity coupling condition, the nonlinear loss due to comb generation and the effective pump detuning are considered in this procedure. Figure 5 (a) shows one comb measured at the through port of a silicon nitride microring resonator which has normal group velocity dispersion. The phase profile is retrieved through spectral line-by-line shaping [45]. A clear phase difference can be observed between the through-port pump and the estimated intracavity pump. Figure 5(b) shows the reconstructed intracavity waveform which is a complex dark pulse.

2.3 Parametric seeding

The microcombs are not always coherent [45], and show rich dynamics and possibilities. In many cases, subcombs with different offset frequencies can be observed [46].

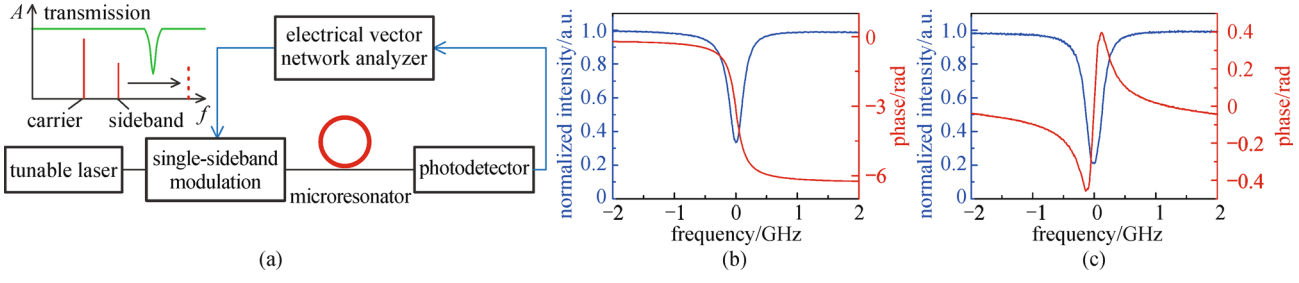

Fig. 4 Testing the microresonator coupling condition. The optical transmission is transferred to the electrical domain by sweeping the microwave modulation frequency. (a) Experimental setup; (b) and (c)examples of measured amplitude and phase responses when the resonance is over-coupled and under-coupled (adapted by permission from Macmillan Publishers Ltd: Nature Photonics [42], copyright 2015)

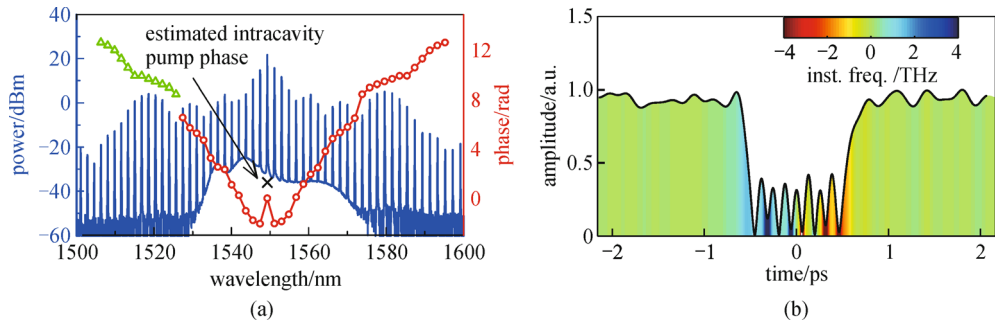

Fig. 5 Reconstruction of the intracavity time-domain waveform through line-by-line shaping and pump correction at a through port. (a) Comb spectrum and phase profile. The red circles are retrieved through line-by-line shaping. The green triangles correspond to additional comb lines that fall outside of the pulse shaper operating band, and are estimated based on symmetry about the pump line. The black cross is the intracavity pump phase estimated by considering the nonlinear loss induced by comb generation and the cold cavity coupling condition; (b) reconstructed intracavity waveform showing a complex dark pulse. Inst. freq.: instantaneous frequency (adapted by permission from Macmillan Publishers Ltd: Nature Photonics [42], copyright 2015)

How to generate wideband coherent equidistant microcombs is an important topic in the research area. A method of parametric seeding was proposed in Ref. [47], which can force coherence through injection locking. Parametric seeding also provides a way to tune the comb line spacing which is an important function for some applications such as optical clocks. Actually one of the early demonstrations of microcomb optical clock is based on parametric seeding [20]. The scheme of the optical clock is shown in Fig. 6(a). An on-chip silica microdisk resonator is used for comb generation. The intensity of the pump laser is modulated by a microwave source. The microwave frequency (f_{eo}) is ~33 GHz, close to the free spectral range of the microdisk. The modulation sidebands are amplified, tailored in a piece of highly nonlinear fiber (HNLF), and then act as an external source to seed the microcomb. Injection locking can be achieved by optimizing the seeding frequency in a region of several hundreds of kHz (see Fig. 6(b)). The subcombs are completely suppressed in the injection locked region and the comb spacing can be tuned directly by changing f_{eo}. The microcomb is amplified and further broadened in a second piece of HNLF (see Fig. 6(c)). To operate an optical clock, two lines of the comb 108 modes apart are phase locked to two distributed feedback (DFB) lasers (D1 and D2) by control of the pump frequency and the intensity modulation frequency. The two DFB reference lasers are stabilized to Rb transitions. The output of the optical clock is obtained via photodetection of the 32.9819213 GHz line

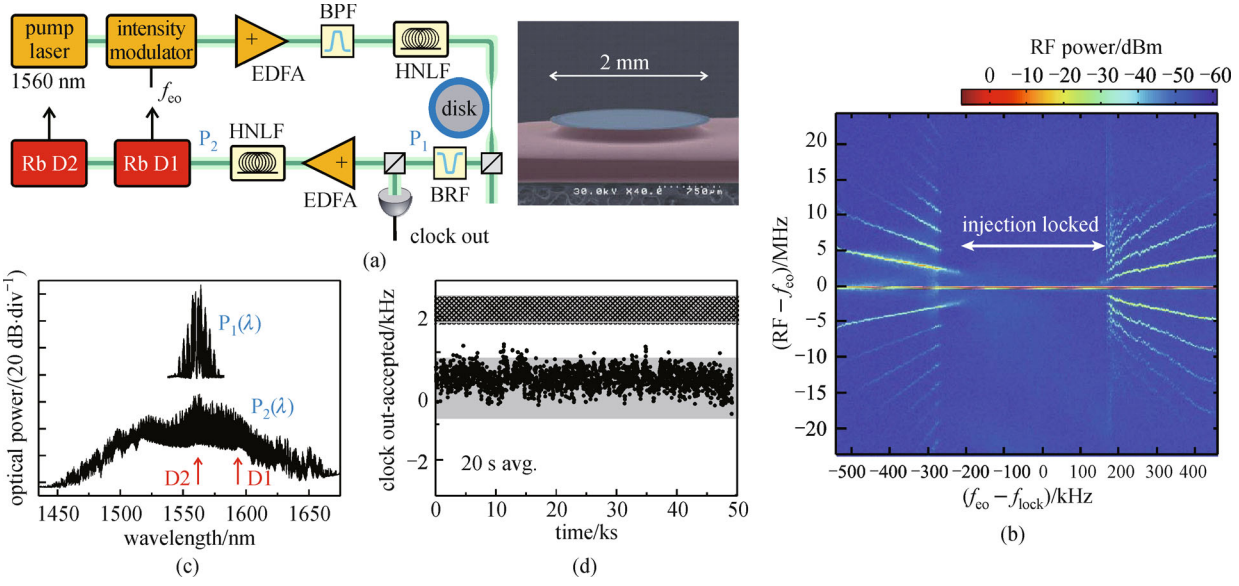

Fig. 6 Optical clock based on parametric seeding of a microcomb. (a) Experimental setup; (b) change of comb line beat notes with the seeding frequency. The region with a single beat note is injection locked; (c) comb spectra after the microdisk resonator (upper) and after the highly nonlinear fiber (HNLF) (lower); (d) optical clock output in a > 12 h period. For comparison, published Rb spectroscopic data on the D2-D1 difference divided by 108 has been subtracted. The solid [48] and hatched [49] gray regions represent previous data (adapted from Ref. [20]). EDFA: erbium-doped fiber amplifier; BPF: bandpass filter; BRF: bandreject filter

spacing, which reflects the frequency difference Δ_{Rb} of the D1 and D2 stabilized lasers divided by 108, and a fixed 660/108 MHz offset for phase stabilization. Figure 6(d) shows the clock output in a > 12 h period. The stability of the clock is at 10^{-9} level with averaging time 0.1 s, which is limited by the stability of the Rb reference.

3 Microcomb generation for microwave photonics

3.1 High spectral purity microwave generation

High spectral purity microwave sources are key elements for many applications including wireless communications, radar, and radio astronomy. Microwave photonic oscillators can potentially achieve superior spectral purity over electronic oscillators. One of the state-of-the-art microwave sources is generated with optical frequency division which is based on the optical frequency comb technique [50]. The high potential of microcombs as ultra-compact microwave photonic oscillators was recognized as early as parametric oscillation was first demonstrated in high-Q nonlinear microresonators [51]. A narrow-linewidth microwave frequency can be obtained by photodetection of the beat note of a coherent microcomb. It has been demonstrated in a recent paper that [21], microcomb-based microwave sources can achieve much better spectral purity than existing microwave photonic oscillators of similar size, weight and power consumption. Figure 7(a) shows the spectrum of the narrow-linewidth 9.9-GHz microwave signal reported in Ref. [21]. The optical spectrum is shown in Fig. 7(b) which is generated from an MgF_2 WGM resonator (intrinsic $Q \sim 5 \times 10^9$). Figure 7(c) shows the single-sideband phase noise of the microwave, which is −60 dBc/Hz at 10 Hz, −90 dBc/Hz at 100 Hz and −170 dBc/Hz at 10 MHz. It is found that the phase noise depends on many parameters including the temperature stability, the pump laser relative intensity noise, the microresonator Q factor, the pump-resonance detuning, the comb mode-locking mechanism, and the shot noise [52–54]. In Fig. 7 (c), the phase noise at small offset frequencies below 1 kHz is limited by fluctuations of the resonator frequency. The noise floor above 10 MHz is limited by the shot noise and can be further reduced by inserting a narrow-band electrical filter after the photodetector. At intermediate frequencies between 1 kHz and 10 MHz, the phase noise is due to a transfer of the laser relative intensity noise to the microwave phase modulation through comb dynamics. The theoretical limits resulting from quantum vacuum fluctuations and thermodynamic fluctuations are much lower than the demonstrated phase noise level. Thus there is still room to further improve the spectral purity by reducing the laser relative intensity noise and employing better thermal and mechanical stabilization of the system.

3.2 Microwave photonic signal processing

One important research topic in microwave photonics is the synthesis of microwave photonic filters (MPFs) which

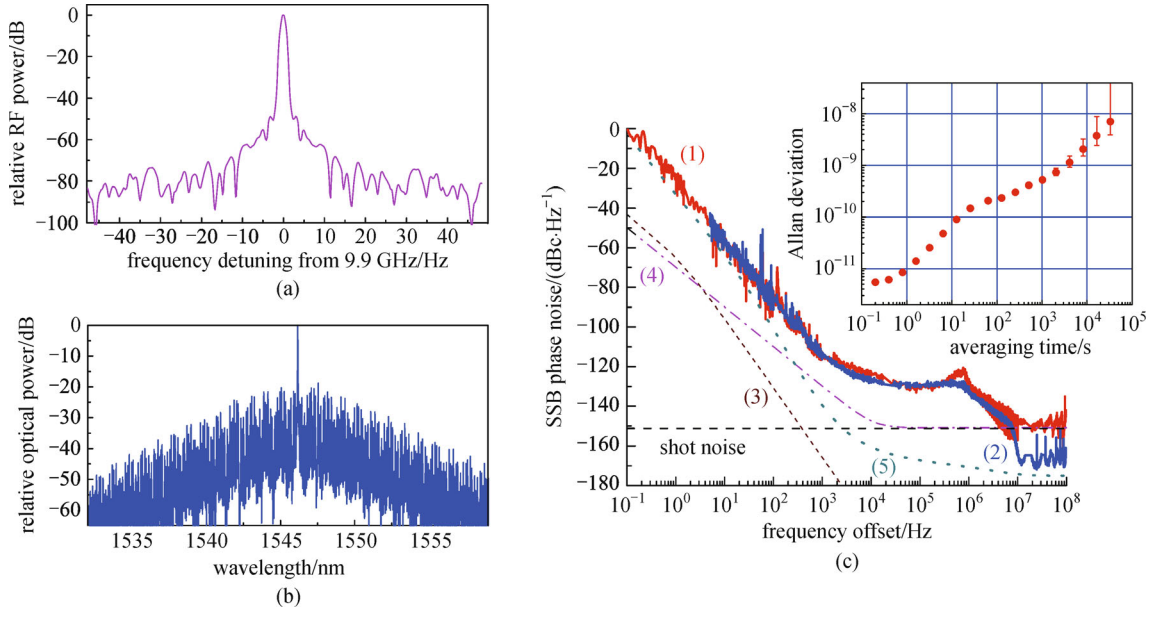

Fig. 7 High spectral purity microwave generation with a microcomb. (a) Spectrum of the microwave signal measured with 9-Hz resolution bandwidth; (b) spectrum of the frequency comb generating the microwave signal; (c) single-sideband (SSB) phase noise of the microwave signal without (red line, (1)) and with (blue line, (2)) a narrow-band radiofrequency filter placed after the photodetector. The measured noise at offset frequencies below 1 kHz and above 10 MHz are within 3 dB of the noise floor of the microwave phase noise measurement system used. The other curves are: (3) theoretical thermo-refractive noise; (4) quantum noise; (5) sensitivity of the phase noise measurement system. The inset shows Allan deviation of the microwave signal (adapted from Ref. [21])

are capable of processing high-frequency microwave signals with photonic devices [55–57]. One most common structure of MPFs is based on multi-wavelength optical sources and dispersive delay lines. The microwave signal to be processed is first converted to multi-wavelength optical signals via modulation of the optical source. The different wavelengths are then tailored, time delayed and photodetected to generate the microwave output. The advantage of this structure is that the microwave transfer function can be programmably controlled by shaping the optical spectrum. Ultrafast tunability can also be achieved with fast electrical phase control [58]. The drawback, however, is the need of a large number of optical wavelengths. Diode laser arrays can be used but the cost is very high. Frequency comb sources can reduce the cost and volume, but traditional mode-locked lasers and electro-optic combs are still quite bulky preventing MPFs from real applications. Microcombs can greatly reduce the volume and cost, thus are very promising for microwave photonic filtering.

The first demonstration of microcomb-based MPF was reported in Ref. [22]. Figure 8(a) shows the experimental setup. A silicon nitride microring resonator (loaded $Q \sim 7 \times 10^5$) is used to generate the frequency comb. The comb spectrum after the microring is shown in Fig. 8(b). The comb is then shaped to a Hamming window (spectrum shown in Fig. 8(c)) and used as the source for the subsequent filtering structure. The filtering is performed with an interferometric structure which can provide complex tap coefficients and high reconfigurability [59]. A piece of single-mode fiber is used as the dispersive delay line. The filter transfer function can be programmed by programming pulse shaper 2 in the interferometer, and the passband center frequency can be tuned by changing the tunable delay line. The maximum microwave frequency that can be handled by a comb-based MPF is limited by one half of the comb line spacing which is generally called the Nyquist zone [60]. One advantage of microcombs is that the comb line spacing can be much higher than traditional mode-locked lasers and electro-optic combs; thus a larger Nyquist zone can be achieved. In the demonstration shown in Fig. 8, the comb line spacing is 231.3 GHz corresponding to a Nyquist zone of 115.6 GHz. Furthermore, the large comb line spacing also makes it possible to use the pulse shaper to suppress unwanted passbands in the optical domain to achieve a real single-

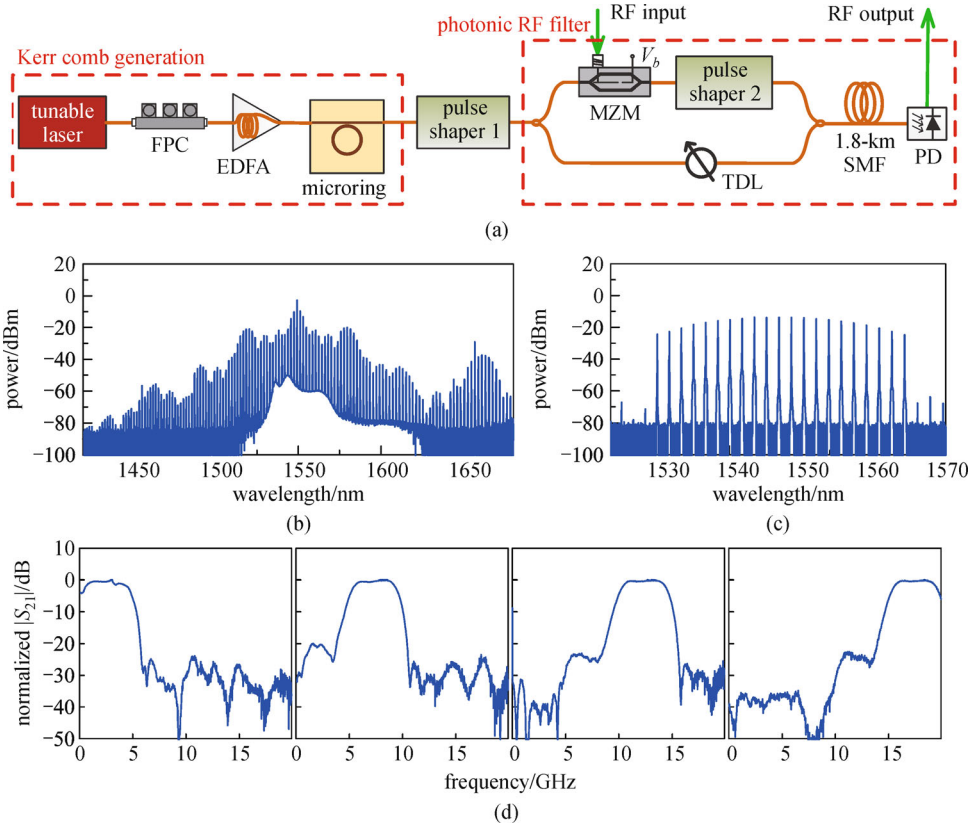

Fig. 8 MPF based on a microcomb. (a) Experimental setup. FPC: fiber polarization controller; EDFA: erbium-doped fiber amplifier; MZM: Mach-Zehnder modulator; TDL: tunable delay line; SMF: single-mode fiber; PD: photodetector; (b) comb spectrum after the microring; (c) shaped comb spectrum after pulse shaper 1; (d) single-passband RF transfer function that is configured to a flat-top by programming pulse shaper 2. The center frequency is tuned between 0–20 GHz by changing the tunable delay line (adapted from Ref. [22])

passband microwave filter. Figure 8(d) shows the measured transfer function when the passband is configured to a flat-top with a bandwidth of 4.3 GHz. The passband center frequency can be continuously tuned between 0 – 20 GHz which is only limited by the frequency response of the modulator and photodetector.

A wideband Hilbert transformer based on the microwave photonic filtering structure was also demonstrated in Ref. [23]. An ideal Hilbert transformer has a flat amplitude transmission in its passband and provides a uniform 90° phase shift to all the frequencies. The microcomb is generated from an integrated Hydex glass microring (loaded $Q \sim 1.3 \times 10^6$). Figures 9(a) and 9(b) show the shaped microcomb spectra with different number of taps for the Hilbert transformer. Figures 9(c) and 9(d) show the measured amplitude and phase responses of the microwave transfer function. The phase response is almost uniform with −90° in a wide range from 0.3 to 16.9 GHz. The amplitude ripples are less than 3 dB and can be further reduced by increasing the number of taps.

4 Discussion

Microcombs have shown great potential as ultra-compact broadband sources for microwave photonic applications. New schemes and functionalities may be made possible by taking advantage of the large line spacing and broad spectra of microcombs. Microcombs are very promising to bring comb-based microwave photonics to real-world applications. To achieve this goal, the performance metrics of the microwave photonic systems need to be investigated and improved more intensely. For example, in the early demonstrations of microcomb-based microwave photonic filtering [22,23], the microwave signal is subjected to a high insertion loss which comes from electro-optical and opto-electrical conversions. The insertion loss can be reduced by improving the comb generation efficiency. This may be possible by improving the microresonator Q factor and optimizing the coupling condition.

Another problem worth concerning is how to integrate the microcombs with the other components, such as pulse shaper, modulator and photodetector, to finally build a compact function module. Currently it is very challenging to monolithically integrate all these different components together because they are generally based on different materials, so system-level integration is the most possible direction. However, it is highly interesting to explore new materials and platforms which can potentially achieve monolithic integration of the whole system.

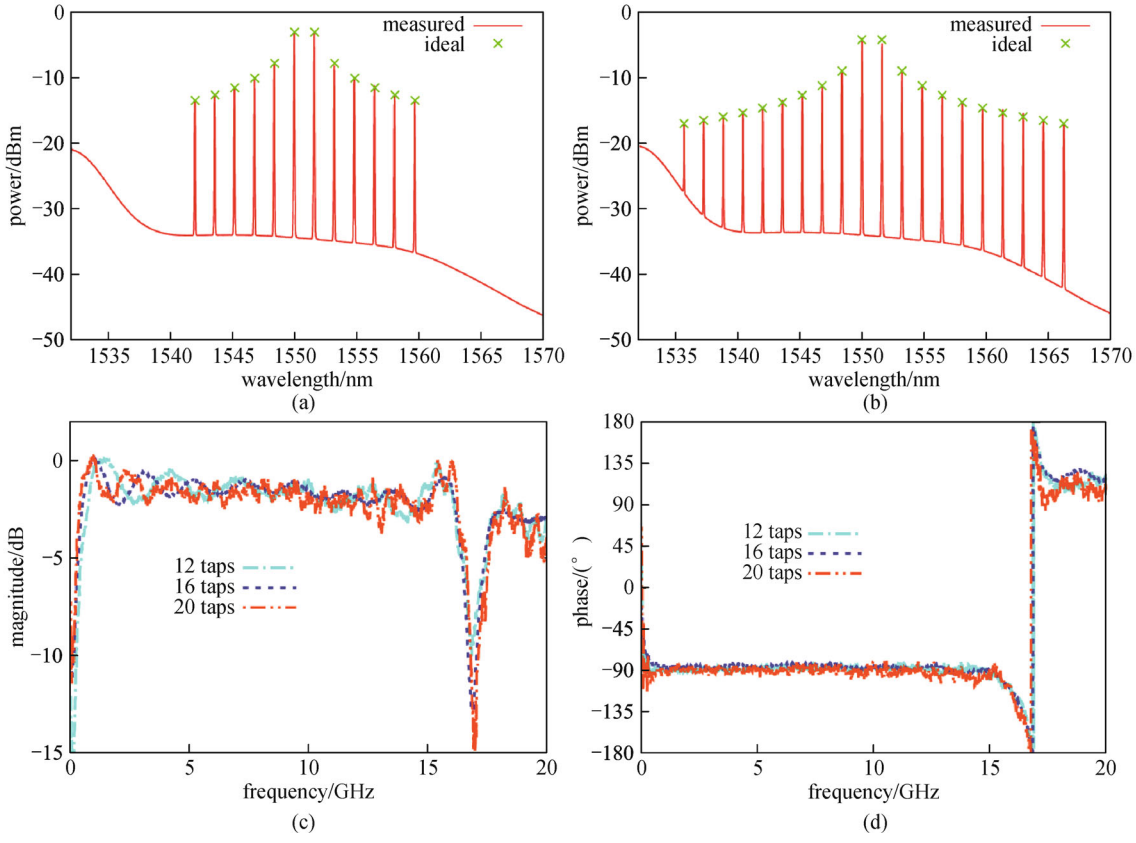

Fig. 9 Wideband Hilbert transformer based on a microcomb. Shaped comb spectrum for (a) 12-tap filter; (b) 20-tap filter; (c) amplitude and (d) phase of the microwave transfer function (adapted from Ref. [23])

Acknowledgements This work was supported in part by the Air Force Office of Scientific Research under grant FA9550-15-1-0211, from the DARPA PULSE program through grant W31P40-13-1-0018 from AMRDEC, and from the National Science Foundation under grant ECCS-1509578.

References

1. Del'Haye P, Schliesser A, Arcizet O, Wilken T, Holzwarth R, Kippenberg T J. Optical frequency comb generation from a monolithic microresonator. Nature, 2007, 450(7173): 1214–1217
2. Del'Haye P, Herr T, Gavartin E, Gorodetsky M L, Holzwarth R, Kippenberg T J. Octave spanning tunable frequency comb from a microresonator. Physical Review Letters, 2011, 107(6): 063901
3. Okawachi Y, Saha K, Levy J S, Wen Y H, Lipson M, Gaeta A L. Octave-spanning frequency comb generation in a silicon nitride chip. Optics Letters, 2011, 36(17): 3398–3400
4. Levy J S, Gondarenko A, Foster M A, Turner-Foster A C, Gaeta A L, Lipson M. CMOS-compatible multiple-wavelength oscillator for on-chip optical interconnects. Nature Photonics, 2010, 4(1): 37–40
5. Razzari L, Duchesne D, Ferrera M, Morandotti R, Chu S, Little B E, Moss D J. CMOS-compatible integrated optical hyperparametric oscillator. Nature Photonics, 2010, 4(1): 41–45
6. Kippenberg T J, Holzwarth R, Diddams S A. Microresonator-based optical frequency combs. Science, 2011, 332(6029): 555–559
7. Papp S B, Del'Haye P, Diddams S A. Mechanical control of a microrod-resonator optical frequency comb. Physical Review X, 2013, 3(3): 031003
8. Savchenkov A A, Matsko A B, Ilchenko V S, Solomatine I, Seidel D, Maleki L. Tunable optical frequency comb with a crystalline whispering gallery mode resonator. Physical Review Letters, 2008, 101(9): 093902
9. Grudinin I S, Baumgartel L, Yu N. Frequency comb from a microresonator with engineered spectrum. Optics Express, 2012, 20 (6): 6604–6609
10. Wang C Y, Herr T, Del'Haye P, Schliesser A, Hofer J, Holzwarth R, Hänsch T W, Picqué N, Kippenberg T J. Mid-infrared optical frequency combs at 2.5 μm based on crystalline microresonators. Nature Communications, 2013, 4: 1345
11. Ilchenko V S, Savchenkov A A, Matsko A B, Maleki L. Generation of Kerr frequency combs in a sapphire whispering gallery mode microresonator. Optical Engineering (Redondo Beach, Calif.), 2014, 53(12):122607
12. Jung H, Xiong C, Fong K Y, Zhang X, Tang H X. Optical frequency comb generation from aluminum nitride microring resonator. Optics Letters, 2013, 38(15): 2810–2813
13. Hausmann B J M, Bulu I, Venkataraman V, Deotare P, Lončar M. Diamond nonlinear photonics. Nature Photonics, 2014, 8(5): 369–374
14. Griffith A G, Lau R K, Cardenas J, Okawachi Y, Mohanty A, Fain R, Lee Y H, Yu M, Phare C T, Poitras C B, Gaeta A L, Lipson M. Silicon-chip mid-infrared frequency comb generation. Nature Communications, 2015, 6: 6299
15. Levy J S, Saha K, Okawachi Y, Foster M, Gaeta A, Lipson M. High-performance silicon-nitride-based multiple-wavelength source. IEEE Photonics Technology Letters, 2012, 24(16): 1375–1377
16. Wang P H, Ferdous F, Miao H, Wang J, Leaird D E, Srinivasan K, Chen L, Aksyuk V, Weiner A M. Observation of correlation between route to formation, coherence, noise, and communication performance of Kerr combs. Optics Express, 2012, 20(28): 29284–29295
17. Pfeifle J, Brasch V, Lauermann M, Yu Y, Wegner D, Herr T, Hartinger K, Schindler P, Li J, Hillerkuss D, Schmogrow R, Weimann C, Holzwarth R, Freude W, Leuthold J, Kippenberg T J, Koos C. Coherent terabit communications with microresonator Kerr frequency combs. Nature Photonics, 2014, 8(5): 375–380
18. Pfeifle J, Coillet A, Henriet R, Saleh K, Schindler P, Weimann C, Freude W, Balakireva I V, Larger L, Koos C, Chembo Y K. Optimally coherent Kerr combs generated with crystalline whispering gallery mode resonators for ultrahigh capacity fiber communications. Physical Review Letters, 2015, 114(9): 093902
19. Savchenkov A A, Eliyahu D, Liang W, Ilchenko V S, Byrd J, Matsko A B, Seidel D, Maleki L. Stabilization of a Kerr frequency comb oscillator. Optics Letters, 2013, 38(15): 2636–2639
20. Papp S B, Beha K, Del'Haye P, Quinlan F, Lee H, Vahala K J, Diddams S A. Microresonator frequency comb optical clock. Optica, 2014, 1(1): 10–14
21. Liang W, Eliyahu D, Ilchenko V S, Savchenkov A A, Matsko A B, Seidel D, Maleki L. High spectral purity Kerr frequency comb radio frequency photonic oscillator. Nature Communications, 2015, 6: 7957
22. Xue X, Xuan Y, Kim H J, Wang J, Leaird D E, Qi M, Weiner A M. Programmable single-bandpass photonic RF filter based on Kerr comb from a microring. Journal of Lightwave Technology, 2014, 32 (20): 3557–3565
23. Nguyen T G, Shoeiby M, Chu S T, Little B E, Morandotti R, Mitchell A, Moss D J. Integrated frequency comb source based Hilbert transformer for wideband microwave photonic phase analysis. Optics Express, 2015, 23(17): 22087–22097
24. Maiman T H. Stimulated optical radiation in ruby masers. Nature, 1960, 187(4736): 493–494
25. Blumenthal R H. Design of a microwave frequency light modulator. Proceedings of the IRE, 1962, 50(4): 452–456
26. Riesz R P. High speed semiconductor photodiodes. Review of Scientific Instruments, 1962, 33(9): 994–998
27. Seeds A J. Microwave photonics. IEEE Transactions on Microwave Theory and Techniques, 2002, 50(3): 877–887
28. Seeds A J, Williams K J. Microwave photonics. Journal of Lightwave Technology, 2006, 24(12): 4628–4641
29. Capmany J, Novak D. Microwave photonics combines two worlds. Nature Photonics, 2007, 1(6): 319–330
30. Yao J. Microwave photonics. Journal of Lightwave Technology, 2009, 27(3): 314–335
31. Capmany J, Li G, Lim C, Yao J. Microwave Photonics: current challenges towards widespread application. Optics Express, 2013, 21(19): 22862–22867
32. Marpaung D, Roeloffzen C, Heideman R, Leinse A, Sales S, Capmany J. Integrated microwave photonics. Laser & Photonics Reviews, 2013, 7(4): 506–538
33. Capmany J, Doménech D, Muñoz P. Graphene integrated microwave photonics. Journal of Lightwave Technology, 2014, 32(20): 3785–3796
34. Marpaung D, Pagani M, Morrison B, Eggleton B J. Nonlinear

integrated microwave photonics. Journal of Lightwave Technology, 2014, 32(20): 3421–3427
35. Optical Frequency Combs. http://www.nist.gov/public_affairs/releases/frequency_combs.cfm
36. Ye J, Cundiff S T. Femtosecond Optical Frequency Comb: Principle, Operation, and Applications. Boston, MA, USA: Springer, 2005
37. Torres-Company V, Weiner A M. Optical frequency comb technology for ultra-broadband radio-frequency photonics. Laser & Photonics Reviews, 2014, 8(3): 368–393
38. Carmon T, Yang L, Vahala K. Dynamical thermal behavior and thermal self-stability of microcavities. Optics Express, 2004, 12(20): 4742–4750
39. Drever R W P, Hall J L, Kowalski F V, Hough J, Ford G M, Munley A J, Ward H. Laser phase and frequency stabilization using an optical resonator. Applied Physics B, Lasers and Optics, 1983, 31 (2): 97–105
40. Black E D. An introduction to Pound–Drever–Hall laser frequency stabilization. American Journal of Physics, 2001, 69(1): 79–87
41. Herr T, Brasch V, Jost J D, Wang C Y, Kondratiev N M, Gorodetsky M L, Kippenberg T J. Temporal solitons in optical microresonators. Nature Photonics, 2014, 8(2): 145–152
42. Xue X, Xuan Y, Liu Y, Wang P H, Chen S, Wang J, Leaird D E, Qi M, Weiner A M. Mode-locked dark pulse Kerr combs in normal-dispersion microresonators. Nature Photonics, 2015, 9(9): 594–600
43. Arcizet O, Schliesser A, Del'Haye P, Holzwarth R, Kippenberg T J. Optical frequency comb generation in monolithic microresonators. In: Matsko A B, ed. Practical Applications of Microresonators in Optics and Photonics . Boca Raton, FL, USA: CRC press, 2009, 483–506
44. Wang P H, Xuan Y, Xue X, Liu Y. Frequency comb-enhanced coupling in silicon nitride microresonators. In: Proceedings of IEEE Conference on Lasers and Electro-Optics (CLEO), 2015
45. Ferdous F, Miao H, Leaird D E, Srinivasan K, Wang J, Chen L, Varghese L T, Weiner A M. Spectral line-by-line pulse shaping of on-chip microresonator frequency combs. Nature Photonics, 2011, 5 (12): 770–776
46. Herr T, Hartinger K, Riemensberger J, Wang C Y, Gavartin E, Holzwarth R, Gorodetsky M L, Kippenberg T J. Universal formation dynamics and noise of Kerr-frequency combs in microresonators. Nature Photonics, 2012, 6(7): 480–487
47. Papp S B, Del'Haye P, Diddams S A. Parametric seeding of a microresonator optical frequency comb. Optics Express, 2013, 21 (15): 17615–17624
48. Marian A, Stowe M C, Lawall J R, Felinto D, Ye J. United time-frequency spectroscopy for dynamics and global structure. Science, 2004, 306(5704): 2063–2068
49. Maric M, McFerran J J, Luiten A N. Frequency-comb spectroscopy of the D1 line in laser-cooled rubidium. Physical Review A., 2008, 77(3): 032502
50. Fortier T M, Kirchner M S, Quinlan F, Taylor J, Bergquist J C, Rosenband T, Lemke N, Ludlow A, Jiang Y, Oates C W, Diddams S A. Generation of ultrastable microwaves via optical frequency division. Nature Photonics, 2011, 5(7): 425–429
51. Savchenkov A A, Matsko A B, Strekalov D, Mohageg M, Ilchenko V S, Maleki L. Low threshold optical oscillations in a whispering gallery mode CaF_2 resonator. Physical Review Letters, 2004, 93 (24): 243905
52. Savchenkov A A, Rubiola E, Matsko A B, Ilchenko V S, Maleki L. Phase noise of whispering gallery photonic hyper-parametric microwave oscillators. Optics Express, 2008, 16(6): 4130–4144
53. Matsko A B, Maleki L. On timing jitter of mode locked Kerr frequency combs. Optics Express, 2013, 21(23): 28862–28876
54. Matsko A B, Maleki L. Noise conversion in Kerr comb RF photonic oscillators. Journal of the Optical Society of America. B, Optical Physics, 2015, 32(2): 232–240
55. Capmany J, Ortega B, Pastor D. A tutorial on microwave photonic filters. Journal of Lightwave Technology, 2006, 24(1): 201–229
56. Minasian R A. Photonic signal processing of microwave signals. IEEE Transactions on Microwave Theory and Techniques, 2006, 54 (2): 832–846
57. Capmany J, Mora J, Gasulla I, Sancho J, Lloret J, Sales S. Microwave photonic signal processing. Journal of Lightwave Technology, 2013, 31(4): 571–586
58. Supradeepa V R, Long C M, Wu R, Ferdous F, Hamidi E, Leaird D E, Weiner A M. Comb-based radiofrequency photonic filters with rapid tunability and high selectivity. Nature Photonics, 2012, 6(3): 186–194
59. Song M, Long C M, Wu R, Seo D, Leaird D E, Weiner A M. Reconfigurable and tunable flat-top microwave photonic filters utilizing optical frequency combs. IEEE Photonics Technology Letters, 2011, 23(21): 1618–1620
60. Hamidi E, Leaird D E, Weiner A M. Tunable programmable microwave photonic filters based on an optical frequency comb. IEEE Transactions on Microwave Theory and Techniques, 2010, 58 (11): 3269–3278

Xiaoxiao Xue received the B.S. and Ph.D. degrees in electronic engineering with the highest honors from Tsinghua University, Beijing, China, in 2007 and 2012, respectively. Since 2013, he has been working as a postdoctoral researcher in the Ultrafast Optics and Optical Fiber Communications Laboratory in Purdue University. His research interests include microresonator-based Kerr comb generation, microwave photonic signal processing, radio over fiber, and phased array antennas. He was a recipient of the 2012 Wang Daheng Prize funded by the Optical Society of China for his Ph.D. dissertation on microwave photonic signal processing.

Andrew M. Weiner graduated from M.I.T. in 1984 with an Sc.D. degree in electrical engineering. Upon graduation he joined Bellcore, first as a Technical Staff Member and later as a Manager of Ultrafast Optics and Optical Signal Processing Research. He moved to Purdue University in 1992 and is currently the Scifres Family Distinguished Professor of Electrical and Computer Engineering. His research focuses on ultrafast optics signal processing and applications to high-speed optical communications

and ultrawideband wireless. He is especially well known for his pioneering work on programmable femtosecond pulse shaping using liquid crystal modulator arrays. He is the author of a textbook entitled Ultrafast Optics and has published more than 250 journal articles. He is a Fellow of the OSA and is a member of the US National Academy of Engineering. He has won numerous awards for his research, including the Hertz Foundation Doctoral Thesis Prize, the OSA Adolph Lomb Medal, the ASEE Curtis McGraw Research Award, the International Commission on Optics Prize, the IEEE LEOS William Streifer Scientific Achievement Award, the Alexander von Humboldt Foundation Research Award for Senior US Scientists, the OSA R.W. Wood Prize, and the IEEE Photonics Society Quantum Electronics Award. He has served as the Chair or Co-Chair of the Conference on Lasers and Electro-Optics, the International Conference on Ultrafast Phenomena and the National Academy of Engineering's Frontiers of Engineering symposium, as the Secretary/Treasurer of the IEEE Lasers and Electro-optics Society (LEOS), and as the Vice-President of the International Commission on Optics (ICO). He is currently the Editor-in-chief of *Optics Express*.